

Development of a new UV resonance Raman spectrometer for the 217–400-nm spectral region

Sanford A. Asher, Craig R. Johnson, and James Murtaugh

Department of Chemistry, University of Pittsburgh, Pittsburgh, Pennsylvania 15260

(Received 23 May 1983; accepted for publication 16 August 1983)

The design and construction of a new UV resonance Raman spectrometer continuously tunable between 217–750 nm are described. The excitation source is based on a YAG laser which is frequency doubled or tripled to pump a dye laser. UV light is generated by nonlinear frequency doubling and mixing of the dye laser output or doubled output with the 1.06- μm YAG fundamental. The detection system utilizes an intensified Reticon multichannel array.

Commercially available monochromators are modified to make them useful for UV resonance Raman spectroscopy. Some sampling methodologies important for UV resonance Raman measurements are described. Examples of the sensitivity of UV resonance Raman spectroscopy are illustrated.

PACS numbers: 07.65.Eh, 82.80.Di, 42.60.Kg, 33.20.Fb

INTRODUCTION

New developments in instrumentation in the late 1960's rekindled interest in the use of Raman spectroscopy as a qualitative and quantitative probe of molecular structure, and as a technique for characterizing sample composition. The first major step towards making Raman spectroscopy a common analytical technique was the development of commercial ion laser sources. The later development of visible wavelength tunable dye lasers initiated a number of studies of the resonance Raman phenomenon in which the Raman spectrum of a molecule is excited at a wavelength within the molecule's electronic absorption band. The resonance phenomenon leads to a significant increase (as much as 10^6) for the Raman intensities of vibrations within the chromaphoric molecular species. This phenomenon leads to a high molecular selectivity in complex systems if the absorption band of an analyte is separate from other absorption bands of other components in the matrix.¹

This selectivity has been used in numerous studies of biological systems. These studies include characterization of heme structure and geometry in heme proteins,^{2,3} elucidation of photochemical reactions of retinal in the visual system,⁴ structural studies of iron sulfur proteins and nucleic acids, as well as for nonbiological inorganic complexes and large conjugated organic molecules.^{1,4,5} In addition to the structural data which can be obtained from the vibrational frequencies, resonance Raman excitation profiles can be used to assign electronic transitions and to determine molecular geometries in excited states.^{6,7}

Almost all previous Raman experiments have been limited to the visible spectral region. Extension of resonance Raman spectroscopy into the UV spectral region was, until recently, limited by the absence of reliable commercially available tunable UV laser sources. However, a few early UV resonance Raman studies utilized excitation at 257 nm from a frequency-doubled high-power Ar⁺ laser.^{8,9} Other studies utilized the fifth harmonic of a Nd-YAG laser at 212.8 nm.¹⁰ A more recent tunable UV resonance Raman spectrometer built by Asher^{11,12} utilized a frequency-doubled flash lamp

dye laser which was tunable from 265–360 nm. This design, which was later directly adopted by others,¹³ utilized a dual PMT–boxcar detection system to simultaneously measure the intensity of the Raman scattered light, as well as the incident laser intensity from the pulsed dye laser. The signal fluctuations due to the pulse-to-pulse intensity fluctuations from the dye laser excitation source were reduced by normalizing the Raman scattered intensity to the incident laser pulse intensity. The tunability of this UV resonance Raman spectrometer was limited to the UV spectral region above 265 nm; the combination of the poor beam quality of flash lamp dye lasers and the fragility and poor efficiency of the doubling crystals used below 260 nm effectively prevent generation of UV light below 260 nm.¹⁴ Another major limitation of this early design was the inability of the dual boxcar integrator detection system to completely compensate for signal fluctuations which result from the pulse-to-pulse intensity fluctuations of the flash lamp dye laser. The dual boxcar detection system will ratio out any linear change in sample signal which results from changes in laser excitation pulse energy, but it cannot ratio out higher order nonlinear signal intensity fluctuations such as those which derive from thermal lensing which result in a detected signal intensity which is not proportional to excitation pulse intensity.

In this report we outline the design of a new UV resonance Raman spectrometer continuously tunable between 217–750 nm. We point out a number of essential features and considerations involved in the construction of the instrument such as multichannel detection and sample handling which are important for successful measurements of UV resonance Raman spectra.

I. INSTRUMENTATION

The excitation source used for the UV resonance Raman spectrometer is a Quanta Ray DCR2A 20-Hz Nd-YAG laser containing both an oscillator and amplifier (Fig. 1). Frequency doubling and tripling crystals supplied in a thermostated, hermetically sealed oven convert the 1.06- μm YAG

UV RAMAN SPECTROMETER

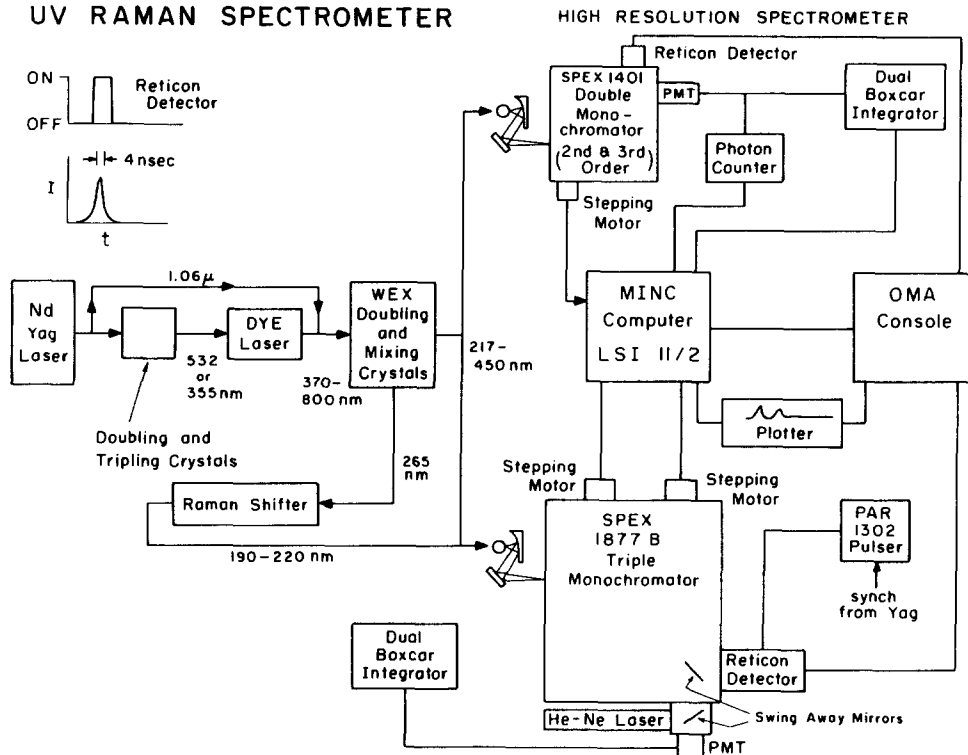


FIG. 1. Block diagram of the UV resonance Raman spectrometer. See text for details.

fundamental to 532- and/or 355-nm light which is used to pump a Quanta Ray PDL dye laser. The dye laser can generate light between 365–750 nm. Tunable light in the UV spectral region is obtained by using harmonic generation techniques such as either mixing the 1.06- μ m YAG output with the dye laser output, doubling the dye laser output or by mixing the doubled dye laser output with the 1.06- μ m YAG fundamental. The doubling and mixing is accomplished using angle-tuned crystals in a Quanta Ray wavelength extender (WEX). The WEX also stabilizes the UV output energy by monitoring the harmonically generated UV beam profile and intensity and, by using a feedback loop, reorients the harmonic generation crystal to maximize the UV output intensity. This active stabilization of the harmonically generated UV power is essential since small temperature changes in the laboratory and within the crystals result in large variations in the harmonic generation efficiency over relatively short time intervals (minutes).

A 20-Hz repetition rate YAG laser was chosen because it provides the maximum UV output power; attempts to achieve higher UV power using a 30-Hz repetition rate YAG laser were unsuccessful because of a decreased crystal harmonic generation efficiency at a 30-Hz repetition rate. The efficiencies of the crystals at 30 Hz are identical to those observed at 20 Hz for the first 10–20 s of dye laser pumping. However, the power then quickly decays to a much lower value. Retuning the crystals will not restore the harmonic generation efficiency. However, the crystal efficiency is restored if the pumping laser is blocked for a few minutes. However, the efficiency quickly decays again after less than one minute of pumping. This phenomenon probably results from a temperature gradient which is set up along the length of the crystal due to absorption of UV light. Because of the temperature dependence of the crystal refractive indices the

temperature gradient prevents phase matching over the entire crystal length which results in a decreased harmonic generation efficiency. Apparently the thermal diffusion rates are too low in these crystals to allow the temperature gradient to decay sufficiently between the 30-Hz pulses.

The output of the doubling and mixing crystals is dispersed by using the WEX Pellin Broca prism. The dye laser fundamental, the YAG 1.06- μ m fundamental and any undesired harmonically generated UV light are spatially rejected within or just outside of the WEX. The desired excitation beam is directed through a diaphragm located about 2 m in front of the WEX and is directed up into the sample compartment by an antireflection coated 90° suprasil quartz prism. The excitation light is focused into the sample by using a 10-in. focusing lens. As the excitation wavelength is altered the Pellin Broca prism is rotated to reestablish the path of the beam through the diaphragm. The small angular misadjustment due any beam displacement at the Pellin Broca prism results in a negligibly small beam displacement at the sample.

The 10-in. focal length lens used for focusing the excitation light in the sample was empirically found to optimize the light collection efficiency while simultaneously keeping the power density in the sample below levels which give rise to nonlinear optical processes such as stimulated Raman scattering. Attempts to temporally stretch the excitation pulse to lower the power density are in progress and will be reported elsewhere.

The choice of sample holders is not critical and we have successfully used stationary suprasil quartz tubes, a rotating suprasil Raman cell and a jet stream. The jet stream apparatus (Fig. 2) was prepared by using a jet nozzle from a Spectra-Physics model 375 dye laser. The stream is rectangular (3-mm high by \sim 0.2-mm wide) and is optically uniform. A

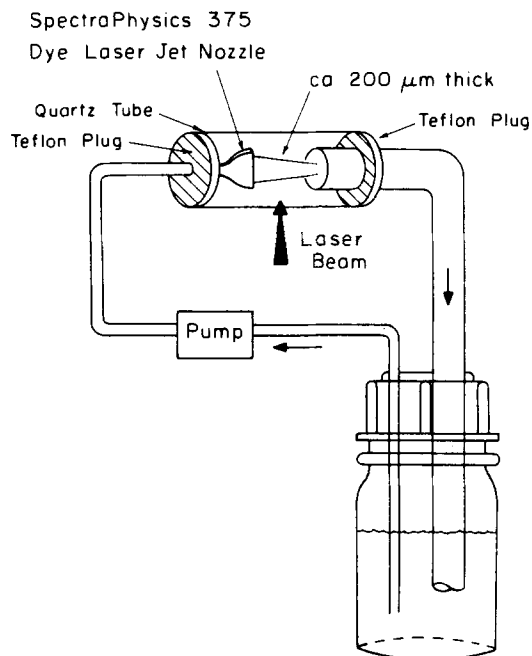


FIG. 2. Sample jet stream assembly.

Teflon stainless-steel centrifugal pump circulates the sample within a closed-loop system which is cooled by ice which surrounds the sample reservoir. A cylindrical quartz tube surrounds the jet to prevent sample evaporation. The outside of the cylinder is slightly heated to prevent condensation of vaporous samples on the walls. The jet stream has a major

advantage because the short sample path length minimizes self-absorption of the resonance Raman scattered light.

The scattered light is collected by using an ellipsoidal mirror and a plane mirror which images the scattered light onto the entrance slit of the monochromator through a crystalline quartz wedge polarization scrambler (Fig. 3). The design of the ellipsoidal mirror collection optics is similar to that previously reported by Asher.¹¹ However, instead of using the aluminum overcoated ellipsoidal mirror designed by Perkin Elmer for their IR spectrometer, the present mirror was obtained from Spex Industries. The surface finish of the new ellipsoidal mirror is superior to the Perkin Elmer mirror. A reference sample chamber and its separate collection optics is mounted perpendicular to the optical axis of the monochromator. For frequency calibration a 45° mirror is inserted to redirect the laser excitation beam to the reference and another 45° mirror is used to redirect the scattered light from the reference onto the entrance slit of the monochromator.

Light was dispersed by using either of two monochromators, a Spex Triplemate 1877B or a modified Spex 1401 double monochromator. The Spex 1401 double monochromator is used for high-resolution studies. The middle slit of the monochromator was removed and replaced by an assembly which accepts a series of slits with fixed jaw spacings. The exit mirror was replaced by a 1-m spherical mirror which images the dispersed light ~25 cm outside the monochromator exit port. A removable 45° mirror mounted in a box attached to the exit port of the Spex 1401 is used to direct the dispersed light to an exit slit for detection by using a

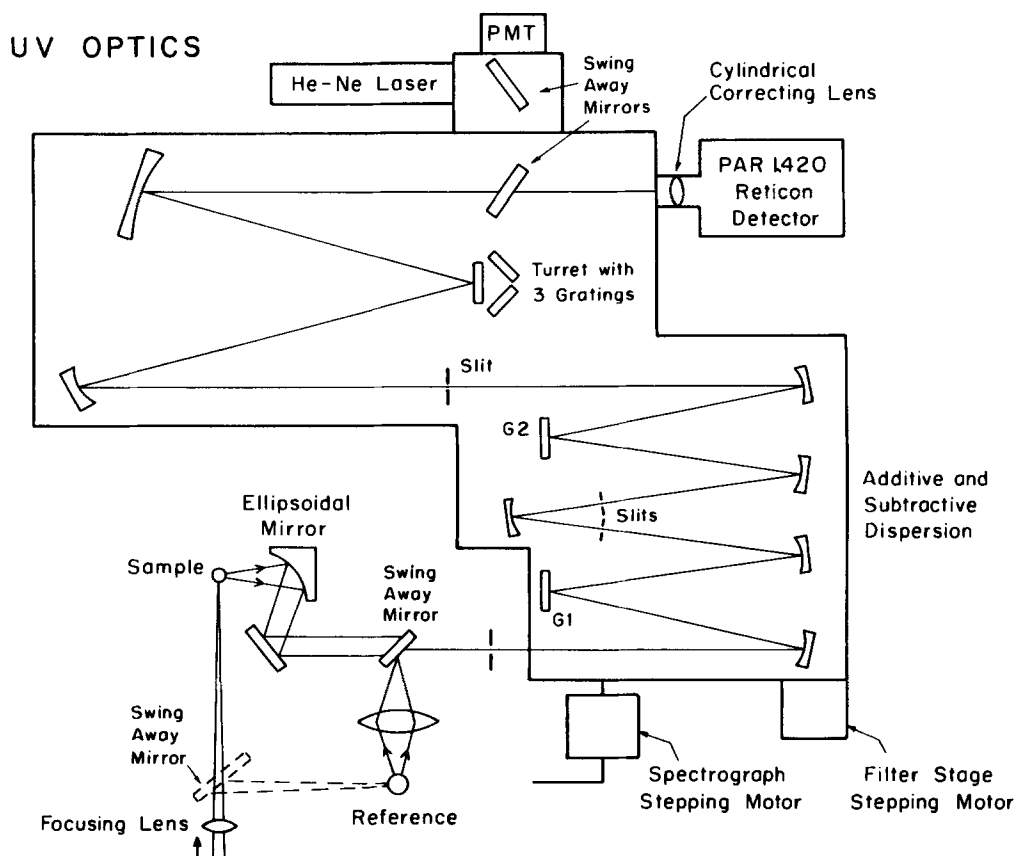


FIG. 3. Sample compartment and optical diagram of the Raman UV spectrometer illustrating the required modifications of the Spex Triplemate monochromator.

photomultiplier and a dual boxcar amplifier or, if the mirror is removed, the dispersed light is imaged onto the photoactive surface of a model 1420 PAR intensified Reticon detector.

The Spex 1401 monochromator is used for high-resolution spectroscopic studies. In the UV spectral region at ~ 250 nm each 1-Å wavelength interval corresponds to 16 cm^{-1} . The modified Spex monochromator has an increased dispersion across the image plane of $\sim 6.4\text{ Å/mm}$ compared to the 5.5-Å/mm dispersion with the original 0.75-m mirror. However, the increased dispersion does not increase the resolution of the monochromator when used with PMT detection because of the accompanying 33% magnification of the entrance slit image. For a $25\text{-}\mu\text{m}$ entrance slit the minimum bandpass remains $\sim 2.2\text{ cm}^{-1}$. In contrast, an increase in resolution does occur for the Reticon detection system since the ultimate resolution limit arises from the effective linear resolution of the Reticon detector. For the Par 1420 Reticon detector the pixel width is $25\text{ }\mu\text{m}$. However due to electronic cross talk between adjacent pixels the effective linear resolution is three pixels, or $75\text{ }\mu\text{m}$. This gives an effective resolution of 6.6 cm^{-1} for the Spex 1401 monochromator when used with slit widths less than $50\text{ }\mu\text{m}$ at ~ 250 nm in first order. This bandpass can be decreased by either using the monochromator in a higher order (i.e., third order gives an $\sim 2.2\text{-cm}^{-1}$ bandpass for 250-nm light) or by magnifying the image using a lens. The limiting resolution of the Spex 1401 for 250-nm light using a $25\text{-}\mu\text{m}$ slit in third order with a lens giving a magnification of three is $\sim 1\text{ cm}^{-1}$. It should be noted that a wavelength drive double monochromator such as the Spex 1400 would permit an even higher resolution since the gratings could be used at even higher orders; the wavenumber drive Spex 1401 is limited in first order using a 1200-groove/mm grating to the 3600-13 000-Å spectral region.

The Spex 1401 monochromator is controlled by a Digital Equipment Corporation Minc LSI 11/02 microcomputer which controls a Superior Electric buffered stepping motor translator which controls a stepping motor externally attached to the lead screw of the Spex 1401 monochromator. The computer also drives a stepping motor which scans the dye laser grating by sending signals through a DRV11 parallel interface to the Quanta Ray MCI-1 dye laser stepping motor controller. As the dye laser grating is rotated, the feedback loop in the WEX automatically reorients the crystals to maximize the UV output energy as the excitation wavelength is scanned.

The dual boxcar detection system is used for the highest resolution Raman studies and for absolute wavelength calibration of the monochromator and the Reticon pixel elements. The design of the boxcar integrator is similar to that previously reported by Asher.¹¹ The outputs of the PMT mounted on the monochromator and the reference PMT which monitors the excitation pulse energy are connected to the inputs of two electrometers through electronic gates which are normally open. These gates are closed during each excitation laser pulse for a $1\text{-}\mu\text{s}$ interval which brackets the laser pulse. The electrometers have a variable 0.5- to 2-s integration time constant. After amplification of the electrom-

eter outputs, an analog output signal proportional to the ratio of the signal intensity to the reference intensity is obtained by using an analog divider. The final output is digitized and stored using an A/D converter on the Minc computer.

The Spex Triplemate monochromator consists of a filter stage which is an additive and subtractive double monochromator (Fig. 3). Light at the laser excitation wavelength is spatially rejected at the intermediate slit in the filter stage. Thus, the input to the spectrograph stage is uniform polychromatic radiation which is dispersed by the spectrograph stage onto the Reticon detector or through a slit to a PMT. The stepping motor normally attached to the Spex 1877B spectrograph stage and an additional stepping motor externally attached to the lead screw of the filter stage permits conventional scanning of the monochromator when using dual boxcar detection. The scanning is controlled by the Minc computer with a DRV11J parallel interface card. The dispersed light is directed to the exit slit and the PMT detector by a removable 45° mirror mounted within the spectrograph stage.

Another removable 45° mirror placed between the exit slit and the PMT permits back illumination of the spectrometer by a He-Ne laser. Optics attached to the He-Ne laser are designed to match the spectrograph f /number. This permits easy alignment of the sample and laser excitation beam prior to a Raman spectral measurement. This is especially important for UV spectral measurements since the image of the scattered light on the slit cannot be visually observed. Generally the monochromator is used with the Reticon detector, in which case the 45° mirror in the spectrograph stage is removed.

The Spex Triplemate monochromator suffers from astigmatism due to its low $f/6.3$ collection optics. In the design of the monochromator the horizontal direction (along the slit width) which determines resolution is corrected for astigmatism. However, the astigmatism is not corrected along the vertical axis which determines the image height. This does not represent a problem for a PMT detector with a large photocathode. However, significant light is lost when using the Reticon detector with its 2.5-mm-high pixel elements. If the entrance slit of the triplemate is illuminated by using a point source imaged at the entrance slit, the height of the image at the image plane of the spectrograph stage is 12 mm due to the astigmatism; different annular segments of the monochromator mirrors focus the vertical axis (slit length) of the image at different positions along on the spectrograph optical axis. Unless an additional optical element is added the 12-mm height of the image overfills the 2.5-mm photoactive reticon height and 80% of the dispersed light is lost. This problem can be obviated by refocusing the vertical axis by using a 1.25-in-diam, 3-in. focal length suprasil cylindrical lens situated ~ 3.5 cm in front of the Reticon detector.

The Reticon detector attaches to the triplemate by using two sliding tubes. The interior tube which has an inside diameter of ~ 1.5 -in. is bolted by using a flange to the spectrograph. The other tube which is attached by a flange to the Reticon slips over the tube attached to the triplemate. The Reticon detector is slid back and forth on these tubes and

rotated in order to place the Reticon photocathode at the spectrograph image plane and to make the length of the pixel elements lie parallel to the slit image. A 1-in. long, $\frac{1}{2}$ -in.-wide slot is cut through the sides of both tubes. This slot is used to position the cylindrical lens. The 1.25-in. cylindrical lens is mounted within a 1.5-in. cylinder which has a threaded hole drilled in its side. The lens and holder are inserted from the inside of the spectrograph through the spectrograph exit port into the tube which couples the Reticon detector to the spectrograph. A threaded rod with a nut is attached to the lens holder through the slot in the side of the coupling tubes. The position of the lens and its orientation is adjusted by the rod to both maximize the spectral resolution and the signal intensity at the Reticon detector.

The ultimate resolution of the Triplemate is limited by the effective $75\text{-}\mu\text{m}$ Reticon resolution element width and the short 0.6-m focal length of the spectrograph stage. In second order at 250 nm the resolution using 1200 groove/mm grating is 8.4 cm^{-1} . However, the 1200-groove/mm grating can be used in third order giving a maximum resolution of $\sim 5.5\text{ cm}^{-1}$. For a $25\text{-}\mu\text{m}$ spectrograph entrance slit

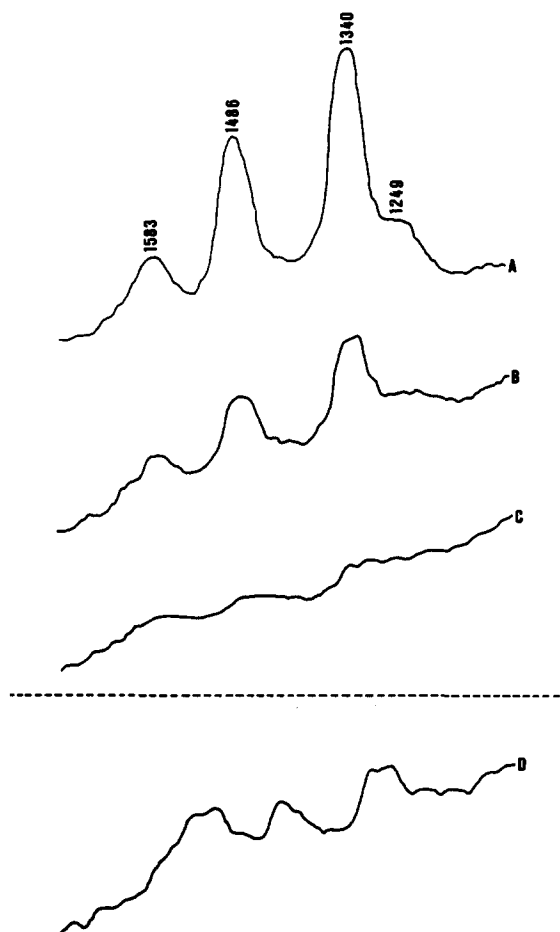


FIG. 4. UV resonance Raman spectra of adenine in water at different adenine concentrations. $\lambda_{\text{ex}} = 252.0\text{ nm}$ at 3-mW power. The adenine concentration is: (A) $9.9 \times 10^{-4}\text{ M}$; (B) $2.0 \times 10^{-4}\text{ M}$; (C) $4.0 \times 10^{-5}\text{ M}$. Each of these spectra were obtained with 10-min scans. Spectrum D is a 20-min scan of the same solution used for C. Spectrum D is plotted on an expanded scale. $\Delta\text{ cm}^{-1}$ values are indicated in spectrum A.

width, replacement of the cylindrical lens with an aspheric lens designed to magnify the horizontal plane by a factor of three could give an ultimate resolution of $\sim 2.7\text{ cm}^{-1}$.

Care must be taken to ensure that the use of higher grating orders does not limit the light throughput due to any polarization bias of the gratings. Particular combinations of orders can lead to essentially zero throughput efficiency for the monochromator. The relative efficiency of any grating is a complicated function of both wavelength and polarization. For example, the efficiency of the Triplemate monochromator using a 600-groove/mm filter stage grating blazed at 5000 \AA in second order and a spectrograph stage 1200-groove/mm grating blazed at 5000 \AA in second order leads to an overall measured efficiency of $\sim 3\%$. In contrast, use of the filter stage gratings in third order while keeping the spectrograph grating in second order leads to an efficiency of less than 0.001%. A polarization scrambler placed in front of the entrance slit to the spectrograph stage effectively avoids these polarization phenomena.

To avoid rf interference from the YAG flash lamp discharge the Reticon detector and the cables are shielded with aluminum foil and grounded at the Reticon 1218 controller. To minimize interference from sample fluorescence the Reticon detector is gated using a PAR 1302 fast pulser. The detector is gated on for a 10-ns interval which brackets the YAG excitation pulse.

The spectrometer was calibrated by using atomic emission lamps. The efficiency of the entire collection optics, monochromator, and detector system was calibrated in the visible spectral region by using a standard intensity incandescent lamp. The UV spectral efficiency was calibrated by using a standard intensity deuterium lamp. The standard intensity light sources were imaged into the monochromator after being scattered from a Lambert surface obtained by spreading Kodak white reflectance standard on a flat plate.

II. RESULTS

Figure 4 shows the resonance Raman spectra of a series of solutions of adenine in water. Each of these spectra were obtained in 10 min (20 min for D) at a 20-Hz laser repetition rate and at an average incident laser power of 0.003 W. The spectra indicate that the resonance enhancement is sufficiently strong with UV excitation to permit vibrational spectral studies in 10^{-6} M solutions. Another important feature of the spectra is that they clearly derive from normal spontaneous resonance Raman scattering and show no contribution from nonlinear stimulated Raman phenomena which could be induced by the high peak power of the 4-ns laser excitation pulses. This conclusion derives from the comparison of the data shown in Fig. 4 with a previously published UV resonance Raman spectrum obtained by frequency doubling a cw high-power Ar^+ laser.¹⁵ All of the peaks show the same relative intensities using the YAG-based laser as in the measurements using a cw doubled Ar^+ laser.

The tunability of this new UV resonance Raman spectrometer permits excitation profile measurements of a variety of compounds. The excitation profile data can be used to examine excited state geometry, to assign absorption bands,

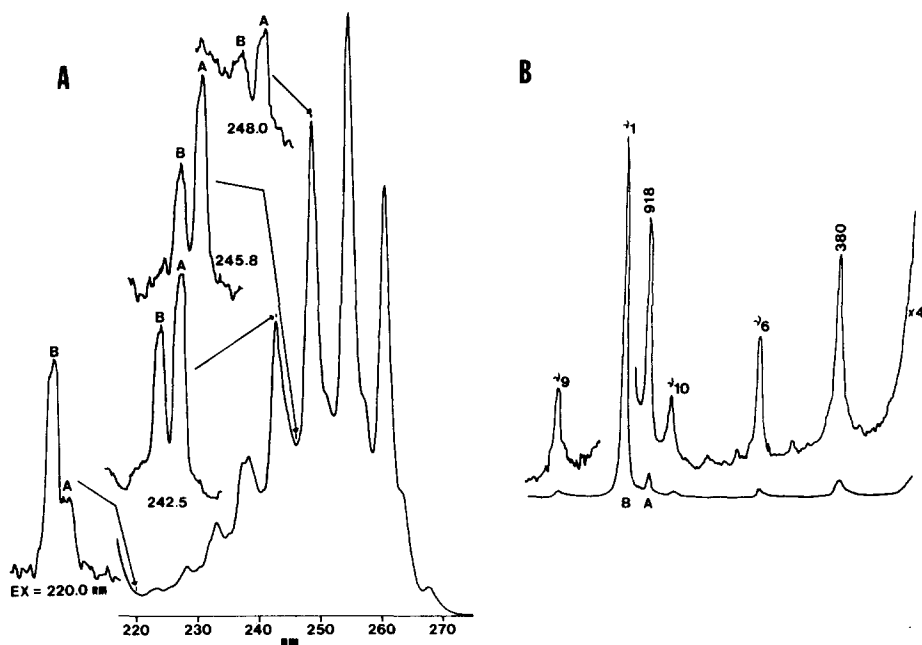


FIG. 5. UV resonance and preresonance Raman spectra of benzene obtained with the instrument described here. (a) UV resonance Raman spectra obtained using the excitation wavelengths as indicated. The 992-cm^{-1} band of benzene and the 918-cm^{-1} band of the solvent (acetonitrile) are shown and labeled B and A respectively. (b) A portion of a preresonance Raman spectrum of benzene obtained with 320.0-nm excitation. Acetonitrile bands are labeled in wavenumbers. The benzene fundamentals are indicated. The resonance Raman spectra were obtained with 1% (V/V) solutions of benzene in acetonitrile. The preresonance Raman spectrum is of a 40% (V/V) solution.

and to study resonance Raman phenomenology. For example, Fig. 5(a) shows the resonance Raman spectra of benzene in acetonitrile excited at 248.0, 245.8, 242.5, and 220.0 nm as well as the absorption spectra of benzene. Figure 5(b) shows a preresonance Raman spectrum at 320 nm excited by our YAG-based system. The absorption spectrum of benzene in Fig. 5(a) indicates the excitation wavelengths used for the Raman spectra shown. The similarity in the relative intensities for the preresonance Raman spectra excited with a 4-ns pulsed YAG-based laser excitation source and Raman spectra of benzene obtained with a cw Ar^+ laser at 4579 \AA in the visible spectral region (not shown) again indicates that nonlinear Raman processes are not occurring. Also the spectra indicate that little fluorescence interference is occurring for the UV resonance Raman measurements.

III. DISCUSSION

An instrument designed for routine UV resonance Raman spectral measurements in the 217–400-nm spectral region has been constructed. The data obtained indicate that UV Raman measurements are easily obtained without interference from sample fluorescence, sample photodecomposition, or nonlinear optical processes. This represents the beginning of a series of UV resonance Raman investigations of molecules absorbing in the UV spectral region. Studies in progress include excitation profile measurements of benzene derivatives, amino acids, and proteins.

ACKNOWLEDGMENTS

We thank Thanh Phung for his machining skills in helping construct the Raman spectrometer. We also gratefully acknowledge support for this study from NSF instru-

mentation grant PCM-8115738 and NIH grant 1R01 GM 30741-01. Acknowledgment is also made to the donors of the Petroleum Research Fund administered by the American Chemical Society for starter grant PRF #13264G46. We also acknowledge starter grant support from a Cottrell Research Corporation Grant and BRSO Grant 2S07 RR 07084-016 awarded by the Biomedical Research Support Grant Program, Division of Research Resources, National Institutes of Health.

- ¹R. J. H. Clark and B. Stewart, *Struct. Bonding (Berlin)* **36**, 1 (1979).
- ²S. A. Asher, *Methods Enzymol.* **76**, 371 (1981).
- ³D. L. Rosseau, J. M. Friedman, and P. F. Williams, *Top. Curr. Phys.* **11**, 203 (1979).
- ⁴P. R. Carey, *Biochemical Applications of Raman and Resonance Raman Spectroscopies* (Academic, New York, 1982).
- ⁵A. T. Tu, *Raman Spectroscopy in Biology: Principles and Applications* (Wiley, New York, 1982).
- ⁶W. L. Peticolas and D. C. Blazej, *Chem. Phys. Lett.* **63**, 604 (1979).
- ⁷E. Suzobi, H. Hamoguchi, H. Haroda, H. Matsuura, and R. Shimanouchi, *J. Raman Spectrosc.* **5**, 119 (1976).
- ⁸I. Harada, Y. Sugawara, H. Matsuura and T. Shimanouchi, *J. Raman Spectrosc.* **4**, 91 (1975).
- ⁹M. Pezolet, T.-J. Uy, and W. L. Peticolas, *J. Raman Spectrosc.* **3**, 55 (1975).
- ¹⁰L. D. Zeigler and B. Hudson, *J. Chem. Phys.* **74**, 982 (1981).
- ¹¹S. A. Asher, Ph.D. thesis, University of California, Berkeley, Lawrence Berkeley Laboratories Report No. LBL-5375.
- ¹²S. A. Asher, L. E. Vickery, T. M. Schuster, and K. Sauer, *Biochemistry* **16**, 5849 (1977).
- ¹³D. C. Blazej and W. L. Peticolas, *Proc. Natl. Acad. Sci. USA* **74**, 2639 (1977).
- ¹⁴S. A. Asher, *Appl. Spectrosc.* (in press 1983).
- ¹⁵A. Laigle, L. Chinsky, and P.-Y. Turpin, *Nucleic Acids Res.* **10**, 1707 (1982).